Scientific Research Publishing

Journal of Materials Science and Chemical Engineering, 2024, 12, 1-17
https://www.scirp.org/journal/msce
ISSN Online: 2327-6053
ISSN Print: 2327-6045

Quantifying Corrosion Rate in Oil and Gas Wells by Measuring Alloying Constituents in Produced Water

Joseph J. Puthuvelil, Fayez A. Al Ammarie, Awad H. Malki

Southern Area Oil Operation Technical Support Department, Saudi Aramco, Dhahran, KSA
Email: joseph.puthuvelil@aramco.com

How to cite this paper: Puthuvelil, J.J., Al Ammarie, F.A. and Malki, A.H. (2024) Quantifying Corrosion Rate in Oil and Gas Wells by Measuring Alloying Constituents in Produced Water. *Journal of Materials Science and Chemical Engineering*, **12**, 1-17.
https://doi.org/10.4236/msce.2024.1212001

Received: October 11, 2024
Accepted: December 1, 2024
Published: December 4, 2024

Abstract

Most oil and gas wells worldwide are completed with low alloy carbon steel due to cost-effectiveness, despite its high susceptibility to corrosion. Corrosion in alloy steels occurs through galvanic or electrolytic reactions, resulting in the release of metallic ions. This release adversely affects the strength and integrity of production tubing. The current study focused on quantifying the amount of alloying constituents present in the produced waters of oil and gas wells using inductively coupled plasma-optical emission spectroscopy (ICP-OES) to calculate the corrosion rate on the production tubing. Two types of alloy steel tubing, API 5CT T-95 and API 5CT J55, were selected. The wells were chosen based on sweet and sour production. The levels of ions present in the produced water—Nickel, Chromium, Manganese, Molybdenum, and Iron—were measured. Ion dissolution was converted to corrosion rate using the exposed area of the tubing and the water flow rate. The study concluded that a very high corrosion rate occurs in sweet wells completed with T-95 metallurgy, whereas the corrosion rate in sour gas producers is significantly less compared to sweet producers. For the oil wells, although they are sour producers, a very low corrosion rate was observed with API 5CT J55 metallurgy. Furthermore, the study revealed that quantifying the alloying constituents in produced water is key to developing suitable corrosion projection approaches, predicting the service life of production tubing in gas and oil wells and metallic structures, and guiding production engineers to make informed decisions and timely responses to corrosion threats before failure.

Keywords

Produced Water, ICP-OES, Ion Dissolution, Alloy Steel, Oil & Gas Wells, Corrosion Rate, Saturation Index

1. Introduction

Due to cost-effectiveness, most gas wells worldwide use low alloy carbon steel, despite its high susceptibility to corrosion [1]. Nevertheless, production tubing corrosion costs the oil and gas industries millions of dollars annually. Corrosion in production tubing occurs via electrochemical processes involving metal oxidation and the corresponding reduction of electrolytic species, resulting in the release of metallic ions [2]. In some cases, corrosion is not limited to electrochemical degradation, as some metal-electrolyte combinations permit chemical dissolution without generating measurable charge [3]. The release of metallic ions can lead to changes in structural characteristics or loss of structural integrity [2].

In fact, well production tubing from the wellhead to the downhole is typically exposed to significant changes in pressure, temperature, water condensation, formation water quality, surface wetting, liquid-to-gas ratio, and other factors, including the presence of acid gases. The rate at which elements are released from the corrosion process under these conditions depends partly on effects associated with passivating film and scale that may form. Therefore, the corrosion of production tubing is a complex, heterogeneous process involving the dissolution and precipitation of multiple solids. Consequently, the condition of the tubing will change considerably, even though the material remains the same. Additionally, two common corrosion mechanisms occur in downhole production tubing, depending on the nature of corrosive gases: sweet corrosion and sour corrosion. Sweet corrosion occurs when metal is exposed to CO_2 or oxygen with water present; sour corrosion occurs when metal is exposed to hydrogen sulfide with water present. Both corrosion mechanisms are influenced by various reservoir parameters such as temperature, partial pressure of corrosive gases, the ratio of H_2S to CO_2, water cut, liquid hydrocarbon production rate, flow rate, flow regime, hydrocarbon type, base metal chemistry, microstructure, cold work, mechanical properties, and etc. [4]. Generally, water itself is not corrosive; however, it plays a significant role in electrochemical reactions when carbon dioxide and hydrogen sulfide are dissolved in it, making the environment acidic [5]. Moreover, in the oil and gas environment, metal surfaces are subjected to mechanical and chemical damage, resulting in susceptibility to electrochemical corrosion.

Corrosion attacks on production tubing in the oil and gas industry are controlled through various preventive measures and monitoring strategies. Preventive measures include design, material selection, protective coating, chemical treatment, and cathodic protection [6]. Another corrosion monitoring strategy is to track the mechanical integrity of subsurface tubulars to maintain gas wells in a safer condition, extend their production life, and prevent communication between the tubing and casing annulus. The corrosion rate of most wells needs close monitoring because, as the field matures, the reservoir produces formation water as a production fluid, leading to higher internal corrosion in the production

tubing. Table 1 shows the main corrosion monitoring strategy adopted by the oil and gas industry and its schedule.

Table 1. Corrosion monitoring test and schedule.

Equipment	Type of protection/Test	Frequency	Data
Production tubing corrosion monitoring at the wellhead, production manifold, and test manifold (immediately downstream)	Coupons	Quarterly	Corrosion rate
	Transmitters/probes connected to the DCS after the wellhead, immediately downstream	Continuous	Corrosion rate
	Planktonic bacteria	Quarterly	Counts
	Sessile bacteria	Quarterly	Counts
	Dissolved Gases (H_2S, CO_2, O_2)	Fortnightly	Quantity
	Iron count	Weekly	Quantity
	Corrosion inhibitor residual	Weekly	Quantity
	Water composition	Monthly	Composition
	Downhole coupon, probes (wireline operation)	As required	Corrosion rate
	Intelligent pigging/Caliper logging	As required	Metal loss (%)

However, conventional corrosion testing methods, such as mass loss and electrochemical testing, do not accurately estimate the true corrosion rate and often obscure the underlying mechanism due to either low sensitivity or a lack of element-resolved analysis [7].

Knowledge of the dissolved constituents in produced water is important because these constituents are related to the origin, disintegration, or degradation of an accumulation. By definition, alloy steel is a mixture of iron and carbon. Steel without added alloy elements is called carbon steel. Carbon steel is used where moderate strength is needed in a non-corrosive environment. When other elements (chromium, molybdenum, nickel, vanadium, manganese, etc.) are added to alter its mechanical and environmental (*i.e.*, corrosion) properties, it becomes alloy steel. Table 2 shows the chemical composition of two alloy steels commonly used in production tubing. API 5CT T-95 alloy steel contains up to 1.5% chromium, 0.85% molybdenum, and 1.2% manganese, while API 5CT J55 contains up to 1.5% manganese, 0.15% chromium, 0.2% nickel, and 0.2% copper. It is hypothesized that if corrosion occurs on alloy steel, significant amounts of some alloying constituents will be released into the water phase. This paper explores an alternative method to monitor corrosion (element-resolved dissolution rate) of production tubing by measuring the alloying constituents in produced water, thus monitoring the corrosion rate in oil and gas wells. We compare two different brands of alloy steel and their tendency toward corrosion by measuring ion release in produced water samples. The dissolved constituents are characterized using the ICP-OES technique in accordance with API RP-45.

Table 2. Typical chemical composition of API 5CT T-95, C90, and API 5CT J55 pipe metallurgy.

	Alloy steel	C	Mn	Mo	Cr	Ni	Cu	Ti	P	S	Si	V	Al
		(%)											
Min	API 5CT T-95	-	-	0.25	0.4		-	-	-	-	-	-	-
Max		0.35	1.2	0.85	1.5	0.99	-	-	0.02	0.01	-	-	-
Min	API 5CT J55	0.34	1.25	-	-	-	-	-	-	-	0.2	-	-
Max		0.39	1.5	-	0.15	0.2	0.2	-	0.02	0.015	0.35	-	0.02

2. Materials and Methods

2.1. Well Selection

A total of 26 gas wells were selected, all completed with API 5CT T-95 tubing. These wells were chosen based on sour gas, condensed water, and a mix of condensed and formation water production. They have been producing sweet and sour gases for the past 5 - 8 years. The sweet wells produce only sweet gases, while the sour gas wells produce sour gases with various H_2S/CO_2 ratios.

Apart from gas wells, 10 oil wells were also selected and completed with API 5CT J55 metallurgy. All the selected wells were sour and formation water producers. The names of the wells selected for this study are shown in Table 3 and Table 4.

Table 3. Wells with condensed water producer.

Sweet Gas wells	Sour Gas wells
API 5CT T-95	API 5CT T-95
SWCT-1	SRCT-1
SWCT-2	SRCT-2
SWCT-3	SRCT-3
SWCT-4	SRCT-4
SWCT-5	

Table 4. Wells with a mix of condensed and formation water producers.

Sweet Gas wells	Sour Gas wells	Sour Oil wells
API 5CT T-95	API 5CT T-95	API 5CT J55
SWMT-1	SRMT-1	SROJ1
SWMT-2	SRMT-2	SROJ2
SWMT-3	SRMT-3	SROJ3
SWMT-4	SRMT-4	SROJ4

Continued

SWMT-5	SRMT-5	SROJ5
SWMT-6	SRMT-6	SROJ6
SWMT-7	SRMT-7	SROJ7
SWMT-8		SROJ8
SWMT-9		SROJ9
SWMT-10		SROJ10

2.2. Element Quantification by ICP OES

The dissolved constituents are characterized using the ICP-OES technique while following API RP-45. Inductively coupled plasma-optical emission spectrometry (ICP-OES) is promising for direct measurements of trace elements within Produced Waters (PWs) with minimal dilution [2]. There are two types of water present upstream of oil and gas pipelines: formation water, which comes from the reservoir wells alongside the hydrocarbons, and condensate water, which forms when the temperature drops below the dew point.

Produced water samples from the wells were filtered to 0.45 μm, acidified in the field to a pH of less than 2 with ultra-pure HNO_3 (Fisher Scientific), and stored at 4˚C in high-density polyethylene bottles [8]. Analysis was performed on a 1 ml aliquot sample, which was diluted to a volume of 10 ml and spiked with an internal standard. The intensity of each emission correlates to the concentration of the corresponding element, allowing for their quantification through a standard calibration procedure. The concentration (CM) is then given by the relationship [9].

$$C_M = \left(I_{\lambda M} - I_{\lambda M}^{\circ}\right) \Big/ k_{\lambda M}$$

where $I_{\lambda M}^{\circ}$ and $k_{\lambda M}$ are the background intensity and the sensitivity factor, respectively, for a given wavelength, λ. This technique offers a large linear dynamic range (LDR, from μg/L to g/L) and excellent detection limits for almost all elements.

Produced water from the wells was analyzed to determine the amounts of Nickel, Chromium, Manganese, Copper, Molybdenum, and Iron using an ICP OES (Agilent Technologies 725). **Table 5** shows the wavelength chosen for each element in ICP to quantify them. Calibration was performed using standard stock solutions (100 mg/mL) prepared by dissolving nitrate salts of the mentioned ions in deionized water. These standard stock solutions were then diluted to achieve the necessary concentrations (0.1 - 10 mg/mL). Once the ICP device was calibrated and a standard calibration curve was obtained, the samples were analyzed along with matrix spikes [10], and the readings were recorded.

TDS (Total Dissolved Solids) of the samples was also determined using the APHA 1030 method.

Table 5. Wavelength and detection limit of elements.

Element	Wavelength (mm)	Detection Limit (μg/L) or (ppb)
Mo	202.032	0.5
Cr	267.716	0.1
Ni	231.604	0.9
Fe	238.204	4.6
Mn	257.610	0.2

2.3. Determination of Corrosion Rate of Metallic Species

Knowing the concentration of the released elements C_M (ppm), the flow rate f (mL/min) and the exposed surface area A (cm^2) allows calculation of the corrosion rate vM (mg/min/cm) of individual elements using the equation below [11]:

$$vM = fC_M / A$$

where it is assumed that M is not present in the initial formation water.

3. Results

3.1. Gas Wells Completed with API 5CT T-95

Dissolution of each metallic species in the alloy steel T-95 was measured using the ICP OES device. The results are illustrated in **Figure 1** and **Figure 2**. The ion concentration was measured for Ni, Cr, Mn, Mo, and Fe for both sweet and sour gas wells. Manganese and iron are the main elements released during the corrosion process, meaning Mn and Fe are selectively dissolved in water compared to other alloying constituents. The overall ion release was greatest for the sweet wells compared to the sour gas wells with T-95 tubular metallurgy. Among the analyzed ions, iron was released the most, followed by Mn; Ni, Cr, and Mo dissolution was negligible. Ion release was significantly lower among wells producing condensed water compared to wells producing formation water.

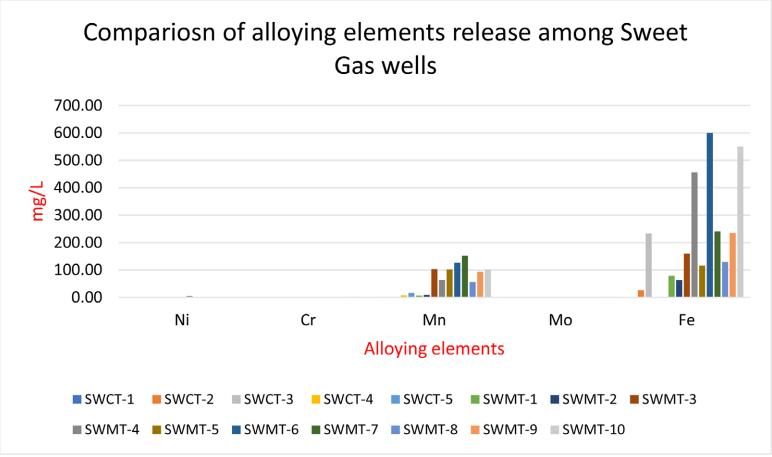

Figure 1. Comparison of alloying element release among Sweet Gas Wells.

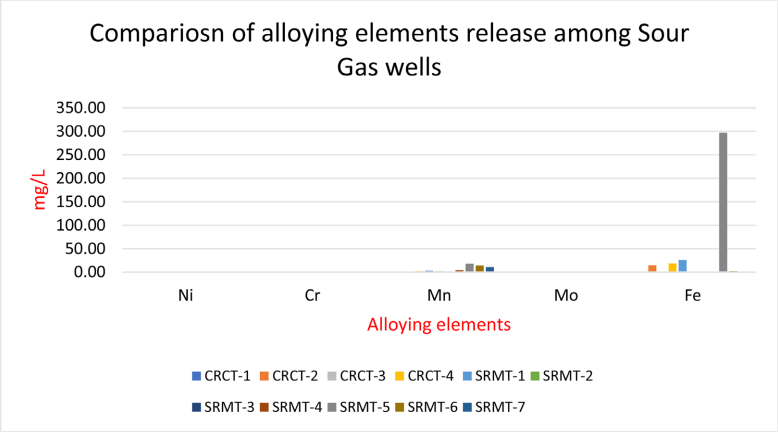

Figure 2. Comparison of alloying element release among Sour Gas Wells.

3.2. Oil Wells Completed with API 5CT J55

For the oil wells, the concentration of alloying elements measured was much lower compared to the gas wells. The results are illustrated in **Figure 3**. The maximum concentration of iron measured at the oil well SROJ1 was 0.57 mg/L, and manganese was 0.74 mg/L.

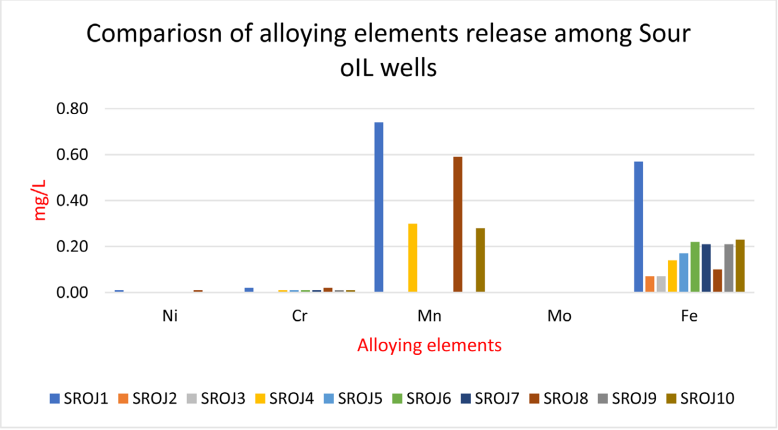

Figure 3. Comparison of alloying element release among Sour Oil Wells.

3.3. Corrosion Rate of Sweet Gas Wells

Shown in **Table 6** is the corrosion rate of sweet gas wells producing condensed water. The data includes the concentration of the released element (CM), water flow rate (f) in mL/min, corrosion rate g/m^2/d, corrosion rate in mills per day (mpy), and corrosion rate in mm/year. In most gas-producing operations, condensed water is available from the start, while formation water follows later. Based on the iron dissolution rate, most wells have a corrosion rate ranging from 0.045 to 2.25 mpy, except for well SWCT-3, which shows 16.23 mpy. Based on the manganese dissolution rate, the corrosion rate for the wells ranges from 0.086 to 0.7 mpy. These results indicate that condensed water promotes only mild corrosion for most wells. For SWCT-3, the corrosion rate based on Mn was only 0.18 mpy.

The higher iron content in SWCT-3 likely comes directly from the formation rock, as this well's target formation is reported to be rich in siderite ($FeCO_3$).

Table 6. Rate of corrosion based on iron and manganese for sweet gas wells with condensed water production.

Sweet Gas wells corrosion rate based on Iron								
S#	Well Name	Type of water	Surface Area of Pipe	Concentration of released element, CM	Water Flow rate, f	Corrosion (mass loss) rate	Corrosion (penetration) rate	Corrosion rate
			A (cm^2)	(mg/L)	(mL/Min)	$g/m^2/d$	mpy	mm/year
1	SWCT-1	Condensed Water	184673443.3	0.32	695.5	0.0246	0.045	0.0012
2	SWCT-2	Condensed Water	191342060.7	26.00	441.6	1.2241	2.240	0.0575
3	SWCT-3	Condensed Water	207081572.9	233.00	386.4	8.8691	16.231	0.4168
4	SWCT-4	Condensed Water	190278757.5	0.18	331.2	0.0064	0.012	0.0003
5	SWCT-5	Condensed Water	193311140.6	2.35	220.8	0.0548	0.100	0.0026
Sweet Gas wells corrosion rate based on Manganese								
S#	Well Name	Type of water	Surface Area of Pipe	Concentration of released element, CM	Water Flow rate, f	Corrosion (mass loss) rate	Corrosion (penetration) rate	Corrosion rate
			A (cm^2)	(mg/L)	(mL/Min)	$g/m^2/d$	mpy	mm/year
1	SWCT-1	Condensed Water	184673443.3	2.50	695.5	0.1921	0.352	0.0090
2	SWCT-2	Condensed Water	191342060.7	1.00	441.6	0.0471	0.086	0.0022
3	SWCT-3	Condensed Water	207081572.9	2.60	386.4	0.0990	0.181	0.0047
4	SWCT-4	Condensed Water	190278757.5	8.00	331.2	0.2841	0.520	0.0134
5	SWCT-5	Condensed Water	193311140.6	16.49	220.8	0.3842	0.703	0.0181

Sweet wells producing a mix of formation and condensed water are shown in Table 7. In these wells, both the Fe and Mn dissolution rates indicate extremely high corrosion. The corrosion rate based on Fe ranges from 30.48 mpy (0.7828 mm/year) to 170.46 mpy (4.3780 mm/year), and based on Mn, it ranges from 2.85 mpy (0.0733 mm/year) to 66.52 mpy (1.7086 mm/year). The dissolution of Fe and Mn and the corresponding corrosion rates reveal extremely high corrosion in these sweet gas producers, which are completed with T-95 metallurgy.

Table 7. Rate of corrosion based on iron and manganese for sweet gas wells with a mix of condensed and formation water production.

Sweet Gas wells based on Iron								
S#	Well Name	Type of water	Surface Area of Pipe	Concentration of released element, CM	Water Flow rate, f	Corrosion (mass loss) rate	Corrosion (penetration) rate	Corrosion rate
			A (cm^2)	(mg/L)	(mL/Min)	$g/m^2/d$	mpy	mm/year
1	SWMT-1	Mix Water	186511251.2	79.00	1927.6	16.6558	30.480	0.7828
2	SWMT-2	Mix Water	180997827.4	63.00	3974.4	28.2208	51.644	1.3264
3	SWMT-3	Mix Water	204731804.2	159.41	3532.8	56.1151	102.691	2.6374
4	SWMT-4	Mix Water	194505715.8	456.00	1324.8	63.3597	115.948	2.9779

Continued

5	SWMT-5	Mix Water	188952910.4	116.13	1656.0	20.7626	37.996	0.9758
6	SWMT-6	Mix Water	204154207.4	600.30	1490.4	89.4011	163.604	4.2019
7	SWMT-7	Mix Water	202999013.9	240.97	1380.0	33.4178	61.155	1.5706
8	SWMT-8	Mix Water	190121231.1	129.36	2152.8	29.8816	54.683	1.4044
9	SWMT-9	Mix Water	183898938.5	235.10	1832.6	47.7948	87.465	2.2464
10	SWMT-10	Mix Water	194151281.4	550.00	1611.8	93.1482	170.461	4.3780

Sweet Gas wells based on Manganese

S#	Well Name	Type of water	Surface Area of Pipe	Concentration of released element, CM	Water Flow rate, f	Corrosion (mass loss) rate	Corrosion (penetration) rate	Corrosion rate
			A (cm^2)	(mg/L)	(mL/Min)	$g/m^2/d$	mpy	mm/year
1	SWMT-1	Mix Water	186511251.2	7.40	1927.6	1.5602	2.855	0.0733
2	SWMT-2	Mix Water	180997827.4	9.10	3974.4	4.0763	7.460	0.1916
3	SWMT-3	Mix Water	204731804.2	103.27	3532.8	36.3528	66.526	1.7086
4	SWMT-4	Mix Water	194505715.8	63.75	1324.8	8.8578	16.210	0.4163
5	SWMT-5	Mix Water	188952910.4	101.77	1656.0	18.1952	33.297	0.8552
6	SWMT-6	Mix Water	204154207.4	126.00	1490.4	18.7649	34.340	0.8819
7	SWMT-7	Mix Water	202999013.9	152.61	1380.0	21.1640	38.730	0.9947
8	SWMT-8	Mix Water	190121231.1	55.50	2152.8	12.8202	23.461	0.6026
9	SWMT-9	Mix Water	183898938.5	94.00	1832.6	19.1098	34.971	0.8982
10	SWMT-10	Mix Water	194151281.4	101.00	1611.8	17.1054	31.303	0.8040

The sweet gas well SWMT-3 exhibited the highest metal loss compared to the other sweet wells. Table 8 shows the pH, TDS, and chloride content in these gas wells. The pH of the sweet gas well samples ranged from 4.4 to 6.1.

Table 8. Sweet gas wells pH, TDS and Chloride.

Well Name	Type of water	pH	TDS	Chloride
			(mg/L)	(mg/L)
SWCT-1	Condensed Water	5.1	706	281.0
SWCT-2	Condensed Water	5.3	650	156.0
SWCT-3	Condensed Water	5.0	674	176.0
SWCT-4	Condensed Water	5.4	895	407.0
SWCT-5	Condensed Water	5.7	2798	1591.0
SWMT-1	Mix Water	6.1	11,388	6529.0
SWMT-2	Mix Water	5.9	13,261	7810.0
SWMT-3	Mix Water	5.9	23,017	13065.0
SWMT-4	Mix Water	4.7	40,721	25618.0

Continued

SWMT-5	Mix Water	4.6	55,175	33813.0
SWMT-6	Mix Water	5.1	59,663	38564.0
SWMT-7	Mix Water	4.5	85,810	52894.0
SWMT-8	Mix Water	5.7	113,665	69800.0
SWMT-9	Mix Water	4.4	116,762	73447.0
SWMT-10	Mix Water	5.3	123,419	79336.0

3.4. Corrosion Rate of Sour Gas Wells

Sour gas wells producing condensed water are shown in Table 9. Based on the iron dissolution rate, most wells have a corrosion rate ranging from 0.006 to 2.07 mpy, except for well SRCT-4, which shows 43.48 mpy. Based on the Mn dissolution rate, the corrosion rate for the wells ranges from 0.008 to 0.25 mpy. The results indicate that condensed water promotes only mild corrosion in most wells. For SRCT-4, the corrosion rate based on Mn was only 0.25 mpy. The higher iron content in SRCT-4 likely comes from the formation rock, as this well's target formation is reported to be rich in siderite ($FeCO_3$). Shown in Table 10 is the rate of corrosion based on iron and manganese for the sour gas wells with a mix of condensed and formation water production. The rate of corrosion is high compared to condensed water producers. This could be due to the combined effect of H_2S, CO_2, Chloride and TDS levels of produced water. Table 11 shows the pH, TDS, and chloride content in these gas wells. The pH results of the samples ranged from 4.6 to 6.4.

Table 9. Rate of corrosion based on iron and manganese for sour gas wells with condensed water production.

Sour Gas wells based on Iron								
S#	Well Name	Type of water	Surface Area of Pipe	Concentration of released element, CM	Water Flow rate, f	Corrosion (mass loss) rate	Corrosion (penetration) rate	Corrosion rate
			A (cm^2)	(mg/L)	(mL/Min)	$g/m^2/d$	mpy	mm/year
1	SRCT-1	Condensed Water	204534896.2	0.17	441.6	0.0075	0.014	0.0004
2	SRCT-2	Condensed Water	183846429.7	14.45	706.6	1.1329	2.073	0.0532
3	SRCT-3	Condensed Water	181,693,569	0.07	419.5	0.0033	0.006	0.0002
4	SRCT-4	Condensed Water	217373297.4	18.50	695.5	23.7594	43.480	1.1167
Sour Gas wells based on Manganese								
S#	Well Name	Type of water	Surface Area of Pipe	Concentration of released element, CM	Water Flow rate, f	Corrosion (mass loss) rate	Corrosion (penetration) rate	Corrosion rate
			A (cm^2)	(mg/L)	(mL/Min)	$g/m^2/d$	mpy	mm/year
1	SRCT-1	Condensed Water	204534896.2	0.10	441.6	0.004404451	0.008	0.0004
2	SRCT-2	Condensed Water	183846429.7	0.20	706.6	0.015680287	0.029	0.0532
3	SRCT-3	Condensed Water	181,693,569	0.60	419.5	0.028261456	0.052	0.0002
4	SRCT-4	Condensed Water	217373297.4	2.10	695.5	0.137073307	0.251	0.0064

Table 10. Rate of corrosion based on iron and manganese for sour gas wells with a mix of condensed and formation water production.

Sour Gas wells based on Iron								
S#	Well Name	Type of water	Surface Area of Pipe	Concentration of released element, CM	Water Flow rate, f	Corrosion (mass loss) rate	Corrosion (penetration) rate	Corrosion rate
			A (cm^2)	(mg/L)	(mL/Min)	$g/m^2/d$	mpy	mm/year
1	SRMT-1	Mix Water	190199994.3	26.00	198.7	0.5542	1.014	0.0260
2	SRMT-2	Mix Water	204705549.8	0.05	4540.8	0.0226	0.041	0.0011
3	SRMT-3	Mix Water	181509788.2	0.01	3974.4	0.0045	0.008	0.0002
4	SRMT-4	Mix Water	189031673.5	0.03	8280.0	0.0268	0.049	0.0013
5	SRMT-5	Mix Water	233230954.4	297.00	4540.8	117.9582	215.864	5.5440
6	SRMT-6	Mix Water	166452890.3	2.09	3974.4	1.0180	1.863	0.0478
7	SRMT-7	Mix Water	173909139.7	0.19	5299.2	0.1181	0.216	0.0056
Sour Gas wells based on Manganese								
S#	Well Name	Type of water	Surface Area of Pipe	Concentration of released element, CM	Water Flow rate, f	Corrosion (mass loss) rate	Corrosion (penetration) rate	Corrosion rate
			A (cm^2)	(mg/L)	(mL/Min)	$g/m^2/d$	mpy	mm/year
1	SRMT-1	Mix Water	190199994.3	3.40	198.7	0.07246698	0.133	0.0034
2	SRMT-2	Mix Water	204705549.8	1.90	4540.8	0.859769301	1.573	0.0404
3	SRMT-3	Mix Water	181509788.2	1.50	3974.4	0.670027998	1.226	0.0315
4	SRMT-4	Mix Water	189031673.5	4.00	8280.0	3.574258151	6.541	0.1680
5	SRMT-5	Mix Water	233230954.4	18.00	4540.8	7.148983026	13.083	0.3360
6	SRMT-6	Mix Water	166452890.3	14.00	3974.4	6.819278643	12.479	0.3205
7	SRMT-7	Mix Water	173909139.7	11.00	5299.2	6.837711246	12.513	0.3214

Table 11. Sweet gas wells: pH, TDS, and Chloride.

Well Name	Type of water	pH	TDS	Chloride
			(mg/L)	(mg/L)
SRCT-1	Condensed Water	4.6	170	44
SRCT-2	Condensed Water	5.5	932	46
SRCT-3	Condensed Water	6.2	1153	361
SRCT-4	Condensed Water	6.4	1665	342
SRMT-1	Mix Water	6.3	6841	3926
SRMT-2	Mix Water	6.1	7647	3919
SRMT-3	Mix Water	5.8	8547	4070
SRMT-4	Mix Water	5.9	9162	5365
SRMT-5	Mix Water	6.3	11,833	6682
SRMT-6	Mix Water	4.6	18,485	11,677
SRMT-7	Mix Water	4.7	507,08	30,493

3.5. Corrosion Rate of Oil Wells

Oil wells producing formation water are listed in Table 12. Results indicate mild corrosion in oil wells completed with J55 metallurgy. Based on the iron dissolution rate, the highest corrosion rate was observed in SROJ5 at 18.51 mpy, while the corrosion rate based on Mn dissolution was negligible. Although all selected oils are sour producers, the overall corrosion rate of the oil wells is comparatively low compared to gas wells. Table 13 depicts the oil wells' corrosion rate based on manganese dissolution. Table 14 shows the produced water's pH, TDS, and chloride content.

Table 12. Oil wells corrosion rate based on iron dissolution.

S#	Well Name	Type of water	Surface Area of Pipe	Concentration of released element, CM	Water Flow rate, f	Corrosion (mass loss) rate	Corrosion (penetration) rate	Corrosion rate
			A (cm^2)	(mg/L)	(mL/Min)	$g/m^2/d$	mpy	mm/year
1	SROJ1	Formation	94489582.4	0.57	2318.4	0.29	0.52	0.01
2	SROJ2	Formation	110,176,586	0.07	129,720	1.68	3.08	0.08
3	SROJ3	Formation	116,989,602	0.07	170899.2	2.09	3.82	0.10
4	SROJ4	Formation	92454866.4	0.14	120115.2	3.71	6.79	0.17
5	SROJ5	Formation	116,503,896	0.17	339811.2	10.12	18.51	0.48
6	SROJ6	Formation	126,165,515	0.22	88099.2	3.13	5.74	0.15
7	SROJ7	Formation	87597802.6	0.21	105100.8	5.14	9.41	0.24
8	SROJ8	Formation	168,211,935	0.10	77,280	0.94	1.72	0.04
9	SROJ9	Formation	170,036,616	0.21	132,480	3.34	6.11	0.16
10	SROJ10	Formation	131,271,996	0.23	88,320	3.16	5.78	0.15

Table 13. Oil wells corrosion rate based on Manganese dissolution rate.

S#	Well Name	Type of water	Surface Area of Pipe	Concentration of released element, CM	Water Flow rate, f	Corrosion (mass loss) rate	Corrosion (penetration) rate	Corrosion rate
			A (cm^2)	(mg/L)	(mL/Min)	$g/m^2/d$	mpy	mm/year
1	SROJ1	Formation	94489582.4	0.34	2318.4	0.17	0.31	0.01
2	SROJ2	Formation	110,176,586	0.00	129,720	0.00	0.00	0.00
3	SROJ3	Formation	116,989,602	0.00	170899.2	0.00	0.00	0.00
4	SROJ4	Formation	92454866.4	0.08	120115.2	2.12	3.88	0.10
5	SROJ5	Formation	116,503,896	0.00	339811.2	0.00	0.00	0.00
6	SROJ6	Formation	126,165,515	0.00	88099.2	0.00	0.00	0.00
7	SROJ7	Formation	87597802.6	0.00	105100.8	0.00	0.00	0.00
8	SROJ8	Formation	168,211,935	0.07	77,280	0.66	1.20	0.03
9	SROJ9	Formation	170,036,616	0.00	132,480	0.00	0.00	0.00
10	SROJ10	Formation	131,271,996	0.15	88,320	2.06	3.77	0.10

Table 14 Oil wells produced water pH, TDS and Chloride content.

S#	Well Name	Type of water	pH	TDS	Chloride
				(mg/L)	(mg/L)
1	SROJ1	Formation water	6.61	72,211	43,521
2	SROJ2	Formation water	6.54	78,456	49,318
3	SROJ3	Formation water	6.74	66,803	41,059
4	SROJ4	Formation water	6.48	86,280	53,060
5	SROJ5	Formation water	6.41	90,616	56,696
6	SROJ6	Formation water	6.62	83,542	51,130
7	SROJ7	Formation water	6.47	73,547	44,074
8	SROJ8	Formation water	6.54	61,698	36,069
9	SROJ9	Formation water	6.40	82,453	49,782
10	SROJ10	Formation water	6.81	47,605	28,306

4. Discussion

The ICP-OES analysis indicated that iron is released in the highest concentration in produced water, followed by Mn. The release of other alloying elements such as Mo, Cr, and Ni is almost negligible, suggesting they are less soluble in the brine and more stable in the oxide formed on the tubular surface. The concentration of released metal ions decreases in the order Fe > Mn > Mo > Cr. The results also show that the relative amounts of released elements from each alloy steel were not proportional to their composition, emphasizing the greater importance of alloy microstructure rather than composition in the dissolution process.

The chemistry of iron compounds is more complex than that of other compounds because iron occurs in water in two oxidation states (Fe^{2+} and Fe^{3+}). Fe^{2+} and Fe^{3+} ions produce compounds with the same anions but widely different solubility. Ni, Cr, and Mo are almost absent in produced water. This is because these metals become inert in acidic environments due to the formation of a passive oxide film on their surfaces, preventing them from dissolving in formation water. Corrosion products like nickel oxide, Cr_2O_3, and molybdenum oxide have low solubility, *i.e.*, the lowest Ksp (solubility product).

In most gas-producing operations, condensed water is present from the beginning, while formation water appears later. Reducing temperature and pressure can produce more condensed water at shallow depths. Condensed hydrocarbons start to form with a decrease in depth, followed by condensed water. As shown in Table 6 and Table 9, condensed water promotes only mild corrosion in both sweet and sour gas wells, ranging from 0.0002 to 0.416 mm/y based on Fe dissolution and 0.002 to 0.25 mm/y based on Mn dissolution. This could be because, even if the condensed water pH is in the acidic range, the total amount of condensed water

is insufficient to promote noticeable corrosion. This suggests that condensed water would not cause significant sweet or sour corrosion to the downhole carbon steel production tubing. In gas wells, sweet or sour corrosion depends on the thickness of the water layer; the thicker it is, the more active the corrosion. Even if condensed water is more corrosive than formation water, it alone would not suffice to promote noticeable sweet or sour corrosion. The observation indicates that downhole corrosion would be marginal in the absence of formation water.

For the sweet gas wells with mixed water producers, a high dissolution rate of Fe and Mn was observed. Dissolving carbon dioxide in water tends to lower the solution's pH by forming carbonic acid, leading to various morphologies of metal dissolution in carbon steel. Two factors may contribute to the higher corrosion rate in these wells: lower pH value and higher chloride concentration in the solution. Chloride ions do not chemically react with the metal but act as a medium or catalyst in the corrosion process. Chloride anions in the solution can help remove the accumulated metal cations by forming soluble compounds, contributing to an accelerated anodic reaction and, thus, faster rusting of the metals. This hypothesis is supported by the research in [12]. The properties of corrosion products are a key factor in controlling downhole corrosion in gas wells. Therefore, corrosion-related workovers may increase in sweet gas operations completed with API 5CT T-95 alloy steel. In other words, corrosion-related workovers might be necessary in less than 10 years of operation with carbon steel completion, assuming formation water breaks out at the onset of the gas stream.

Most of the sour gas producers in this study have not shown a high metal dissolution rate compared to sweet gas wells. The predominance of metal ions in formation water depends on several factors, including pH, Eh (redox potential), partial pressure of dissolved gases (H_2S, CO_2, etc.), and the temperature of the formation water. Unlike sweet gas wells, which produce only sweet gases, sour gas wells produce sour gases with various ratios of H_2S/CO_2. Previous studies have established that H_2S is an effective film-forming agent on carbon steel in high-temperature sour gas wells [13]. Unlike sweet corrosion, sour weight loss corrosion is strongly influenced by the passivity and wettability of corrosion products. In typical sour gas-producing wells, three different groups of corrosion products are thermodynamically present on carbon steel: iron sulfide, iron carbonate ($FeCO_3$), and iron oxide (Fe_3O_4, magnetic). This is because the activity of dissolved oxygen is almost negligible in the produced fluids. Among these, iron sulfide is the predominant corrosion product in sour service due to its low solubility, which is much less than that of iron carbonate or magnetite. Generally speaking, sour weight loss corrosion of carbon steel is an order of magnitude less than that of sweet corrosion. Iron sulfide films can provide varying degrees of protection depending on the H_2S/CO_2 ratio [14]. Injecting hydrogen sulfide gas into water quickly passivates a carbon steel surface, drastically reducing the metal dissolution rate. With an increase in the partial pressure of hydrogen sulfide, the iron sulfide film becomes more stable, effectively suppressing metal dissolution to a certain

degree. H_2S is an effective film-forming agent on carbon steel in high-temperature sour gas wells, controlling the corrosion activity of carbon steel [13]. Iron sulfide corrosion products on carbon steel tubing and pipelines can be protective, but localized corrosion may occur with oxygen ingress, elemental sulfur, or microbial activity [15]-[18]. Alloying elements like Cr, Ni, and Mo can reduce metal dissolution in sour service and improve resistance to sour weight loss corrosion. The production tubing made with API 5CT T-95 carbon steel remains cost-effective in most sour gas wells.

For the oil wells, ion dissolution data and the corresponding corrosion rate revealed that mild corrosion is occurring. Tubing completed with API 5CT J55 is either resistant to corrosion or the FeS coating formed on the surface of the tubing is preventing further corrosion. This observation is clearly justified, as some oil wells in this study have been in production for the last three decades without any corrosion-related maintenance activities.

5. Conclusions

The aim of this study is to utilize metal dissolution in produced water to quantify the corrosion rate, assuming the metal is not present in the initial formation water. Alloying constituents like manganese and iron are identified as options for monitoring oil and gas wells completed with low alloy carbon steels. Among the five alloying constituents measured, the dissolution rates of manganese and iron provide a clear understanding of corrosion and offer an alternative method to measure the corrosion rate without relying on any assumptions. This approach offers an alternative way to monitor corrosion in oil and gas wells, especially when some gas wells cannot perform MIT logs due to $FeS/CaCO_3$ scales, which limit well access and increase operational risk. Additionally, measuring alloying constituents in produced water helps monitor corrosion occurring behind scale buildup in the tubing. This can reduce the need for caliper jobs, particularly for monitoring/time-lapse logs, by calculating the corrosion rate and predicting the tubing's lifetime.

The application of ICP-OES methodology for corrosion rate assessment has significant advantages compared to other methods of corrosion determination.

1) Determining exact corrosion rates is possible without any assumptions.

2) The corrosion rate is determined using precise information about the dissolution of each metallic species in the alloy.

3) The corrosion rate can be measured instantaneously, unlike methods such as mass loss, which require a long time or are not applicable to passive systems with low dissolution rates.

4) Knowing the downhole corrosively helps determine the timing of corrosion-related workovers to avoid expensive fishing operations.

Acknowledgements

The authors would like to thank the management of Saudi Aramco for granting

permission to publish this paper.

Conflicts of Interest

The authors declare no conflicts of interest regarding the publication of this paper.

References

[1] Ameh, E.S. and Ikpeseni, S.C. (2018) Pipelines Cathodic Protection Design Methodologies for Impressed Current and Sacrificial Anode Systems. *Nigerian Journal of Technology*, **36**, 1072-1077. https://doi.org/10.4314/njt.v36i4.12

[2] Jubb, A.M., Engle, M.A., Chenault, J.M., Blondes, M.S., Danforth, C.G., Doolan, C., *et al.* (2020) Direct Trace Element Determination in Oil and Gas Produced Waters with Inductively Coupled Plasma-Optical Emission Spectrometry: Advantages of High-Salinity Tolerance. *Geostandards and Geoanalytical Research*, **44**, 385-397. https://doi.org/10.1111/ggr.12316

[3] Turner, B. (2007) Macedonia. In: *The Stateman's Yearbook*, Palgrave Macmillan UK, 810-813. https://doi.org/10.1007/978-1-349-74024-6_212

[4] Choi, H.J., Al-Tammar, J.I., Zbitowsky, R.L. and Ginest, N.H. (2010) Field Corrosion Investigation of API 5CT T-95 Carbon Steel Production Tubing in Sweet and Sour Gas Wells in Saudi Arabia. 13*th Middle East Corrosion Conference and Exhibition*, Manama, 14-17 February 2010.

[5] Sammimi, A. (2012) Causes of Increased Corrosion in Oil and Gas Pipelines in the Middle East. *International Journal of Basic and Applied Sciences*, **1**, 572-577.

[6] Agarwal, S., Kumar, S., Agarwal, M. and Kamal, M. (2015) Corrosion: A General Review. *Internal Conference of Advance Research and Innovation*, India, 17-18 November 2015, 181-183.

[7] Choudhary, S., Ogle, K., Gharbi, O., Thomas, S. and Birbilis, N. (2022) Recent Insights in Corrosion Science from Atomic Spectroelectrochemistry. *Electrochemical Science Advances*, **2**, Article e2100196. https://doi.org/10.1002/elsa.202100196

[8] Engle, M.A., Reyes, F.R., Varonka, M.S., Orem, W.H., Ma, L., Ianno, A.J., *et al.* (2016) Geochemistry of Formation Waters from the Wolfcamp and "Cline" Shales: Insights into Brine Origin, Reservoir Connectivity, and Fluid Flow in the Permian Basin, USA. *Chemical Geology*, **425**, 76-92. https://doi.org/10.1016/j.chemgeo.2016.01.025

[9] Thompson, M. and Walsh, J.N. (1989) Introduction. In: *Handbook of Inductively Coupled Plasma Spectrometry*, Springer, 1-15. https://doi.org/10.1007/978-1-4613-0697-9_1

[10] Blondes, M.S., Gans, K.D., Engle, M.A., Kharaka, Y.K., Reidy, M.E., Saraswathula, V., Thordsen, J.J., Rowan, E.L. and Morrissey, E.A. (2018) U.S. Geological Survey National Produced Waters Geo-Chemical Database (Ver. 2.3, January 2018). U.S. Geological Survey Data Release. https://doi.org/https://doi.org/10.5066/F7J964W8

[11] Ogle, K. (2012) Atomic Emission Spectro Electrochemistry: A New Look at the Corrosion, Dissolution & Passivation of Complex Materials Corros. *Mater*, **37**, 58-65.

[12] Xi, Y. and Xie, Z. (2002) Corrosion Effects of Magnesium Chloride and Sodium Chloride on Automobile Components University of Colorado, Department of Civil Environmental and Architectural Engineering.

[13] Kvarekval, J., Nyborg, R. and Choi, H.J. (2003) Formation of Multilayer Iron Sulfide Films during High Temperature CO_2/H_2S Corrosion of Carbon Steel. Paper No.0339.

[14] Choi, H.J. and Al-Ajwad, H.A. (2008) Flow-Dependency of Sour Corrosion of

Carbon Steel Production Tubing in Khuff Gas Wells. Paper No. 08638.

[15] Smith, S.N. (1993) A Proposed Mechanism for Corrosion in Slightly Sour Oil and Gas Production. 12*th International Corrosion Congress*, Houston, 19-24 September 1993, 2695-2706.

[16] Wikjord, A.G., Rummery, T.E., Doern, F.E. and Owen, D.G. (1980) Corrosion and Deposition during the Exposure of Carbon Steel to Hydrogen Sulphide-Water Solutions. *Corrosion Science*, **20**, 651-671. https://doi.org/10.1016/0010-938x(80)90101-8

[17] Rhodes, P.R. (1996) Corrosion Mechanism of Carbon Steel in Aqueous H_2S Solution. Extended Abstract No. 107. *Electrochemical Society*, **76**, Article No. 2.

[18] Shoesmith, D.W., Taylor, P., Bailey, M.G. and Owen, D.G. (1980) The Formation of Ferrous Monosulfide Polymorphs during the Corrosion of Iron by Aqueous Hydrogen Sulfide at 21˚C. *Journal of The Electrochemical Society*, **127**, 1007-1015. https://doi.org/10.1149/1.2129808